Deformation and Failure of Graphene Sheet and Graphene-Polymer Interface

Mingchao Wang[1], Cheng Yan[1,*], Ning Hu[2]

[1] School of Chemistry, Physics and Mechanical Engineering, Science and Engineering Faculty, Queensland University of Technology, 2 George Street, GPO Box 2434, Brisbane, Australia
[2] Department of Mechanical Engineering, Chiba University, Inage-ku, Chiba, Japan
* Corresponding author: c2.yan@qut.edu.au

Abstract With a monolayer honeycomb-lattice of sp^2-hybridized carbon atoms, graphene has demonstrated exceptional electrical, mechanical and thermal properties. One of its promising applications is to create graphene-polymer nanocomposites with tailored mechanical and physical properties. In general, the mechanical properties of graphene nanofiller as well as graphene-polymer interface govern the overall mechanical performance of graphene-polymer nanocomposites. However, the strengthening and toughening mechanisms in these novel nanocomposites have not been well understood. In this work, the deformation and failure of graphene sheet and graphene-polymer interface were investigated using molecular dynamics (MD) simulations. The effect of structural defects on the mechanical properties of graphene and graphene-polymer interface was investigated as well. The results showed that structural defects in graphene (e.g. Stone-Wales defect and multi-vacancy defect) can significantly deteriorate the fracture strength of graphene but may still make full utilization of corresponding strength of graphene and keep the interfacial strength and the overall mechanical performance of graphene-polymer nanocomposites.

Keywords Graphene, structural defect, fracture strength, graphene-polymer interface, load transfer

1. Introduction

Graphene has attracted increasing research effort since its discovery [1], largely due to its excellent electrical, mechanical and thermal properties. For example, graphene has high electron mobility (25000 cm^2/Vs) at room temperature [1], anomalous quantum Hall effect [2], extremely high Young's modulus (~1TPa) and fracture strength (~130 GPa) [3] and superior thermal conductivity (5000 $Wm^{-1}K^{-1}$) [4]. These exceptional properties make graphene an ideal candidate as reinforcement in functional and structural polymer composites. For instance, graphene-polymer composite has a electrical conductivity of ~0.1 Sm^{-1} when adding only 1 v% graphene [5]. Poly(acrylonitrile) with 1 wt% functionalized graphene obtains a remarkable shift in glass transition temperature of over 40 °C [6]. More significantly, the composites show notable improvement in fracture strength and toughness, buckling and fatigue resistance [7-12].

Graphene can be produced via chemical vapour deposition (CVD) [13], mechanical exfoliation [14], chemical reduction of graphene oxide sheets [15], etc. It has been confirmed the properties of graphene can be modified by chemical functionalization [16-18]. However, both material production processes and chemical treatment may introduce structural defects in graphene, such as Stone-Wales (S-W) type defects (nonhexagonal rings generated by reconstruction of graphene lattice) [19], single and multiply vacancies, dislocation like defects, carbon adatoms, or accessory chemical groups. Recently, Gorjizadeh et al. [20] demonstrated that the conductance decreases in defective graphene sheets. Pei et al. [21, 22] studied the influence of functionalized groups on mechanical properties of graphene. Furthermore, it is still not well understood the underlying strengthening and toughening mechanisms of graphene-polymer nanocomposites and the influence of defective graphene on them. Further study is much required. Due to the nano-scale dimensions, it is difficult to accurately evaluate the properties of graphene sheets via experiment. Alternatively, molecular dynamics (MD) method has been widely utilized to investigate carbon-based nanomaterials [23-27]. In this work, we present a MD investigation on the fracture strength of graphene with structural defects (S-W defect and multi-vacancy defect) and interfacial behaviour of

graphene-polymer nanocompsites. Our results are helpful for a better understanding of the design and performance of graphene-polymer nanocomposites.

2. Models and Methods

To simulate a monolayer graphene sheet, a MD model (42.6 Å × 49.2 Å) was built that consists of 800 carbon atoms. As confirmed by Zhao et al. [28], the possible model size effect on mechanical properties can be largely neglected when the diagonal length is over 5 nm. Therefore, the diagonal length of our model was chosen as 6.51 nm. The model was firstly relaxed to a minimum energy state with the conjugate gradient energy minimization. Then, Nose-Hoover thermostat [29, 30] was employed to equilibrate the graphene sheet at a certain temperature with periodic boundary conditions (PBCs). The adaptive intermolecular reactive bond order (AIREBO) potential [31] implemented in the software package LAMMPS [32], was used to simulate covalent bond formation and bond breaking. Such AIREBO potential has successfully simulated and predicted mechanical properties of carbon-based materials, i.e. fullerene, carbon nanotube and graphene.

In order to prepare the atomistic structures of graphene-polymer nanocomposite for simulation, a two-dimensional (2D) periodic model of polyethylene (PE) layer independent of graphene nanofiller was established. The polymer system consists of 25 PE molecules, with each molecule (CH_3-(CH2-CH2)$_{59}$-CH_3) composed of about 60 monomers. All the PE chains were prepared by commercial software Material Studio developed by Accelrys Inc. Then, two types of graphene-PE unit cells were constructed by stacking two PE layers with single graphene sheet (Case 1) and single defective graphene sheet (Case 2). To investigate the interfacial characteristics of graphene-PE nanocomposite, an ab initio force filed polymer consistent force field (PCFF) [33, 34] was employed with the effective open-source code LAMMPS [32]. The interfacial interaction has been widely investigated in carbon-based materials and polymer-matrix nanocomposites [35-41]. To obtain the equilibrated structure of such unit cell, the model was first put into a constant-temperature, constant-pressure (NPT) ensemble for 250 ps by fixing the graphene with temperature of T=100 K, pressure of P=1 atm and time step of Δt=1 fs after initial energy minimization (stage 1). Then, the unit cell model was further equilibrated for 250 ps with the same NPT ensemble and time step (stage 2). For the pull-out simulation of graphene from PE matrix, the displacement increment along the x axis of Δx=0.001 Å was applied. During such process, graphene nanofiller were fixed while PE matrix was relaxed to equilibrate the whole dynamic system.

3. Results and Discussion

3.1 Effect of Stone-Wales (S-W) on Fracture Strength

Due to the short-ranged covalent bonding between carbon atoms, bond rotation and bond breaking are two basic deformation mechanisms in graphene. In this study, we considered two types of S-W defects, namely S-W_1 and S-W_2, which are caused by 90° rotation of C-C bonds in different directions, as shown in Figure 1(a). Figure 1(b) showed corresponding stress-strain curves at different temperatures (300 K~900 K). In terms of true (Cauchy) stress, fracture strengths along armchair and zigzag directions at 300 K are 104 and 127 GPa, respectively. These values are in good agreement with experiment results $\sigma_f \approx$130 GPa [3], as well as previous atomistic simulation results [26, 28].

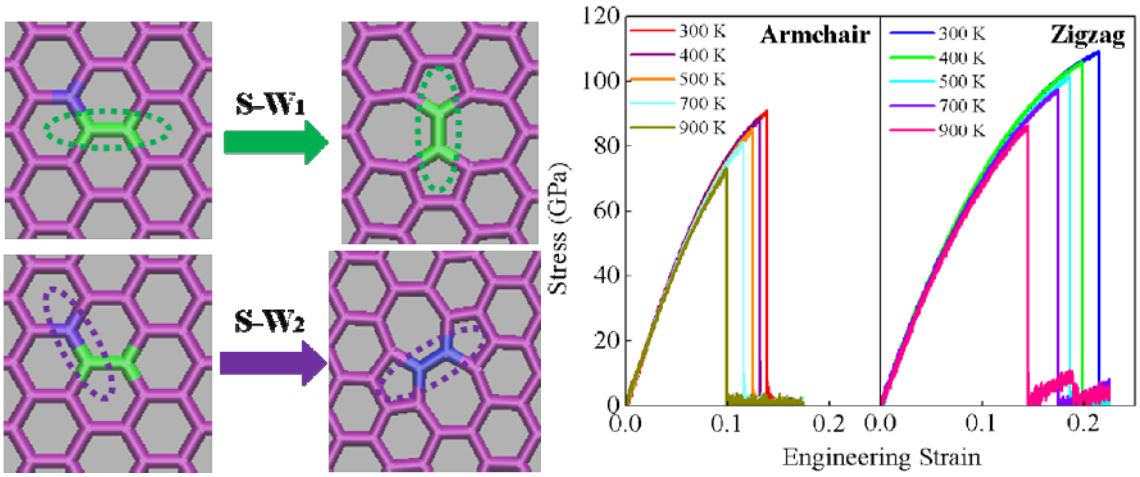

Figure 1. (a) Atomistic models of S-W_1 and S-W_2 defects. (b) Stress-strain curves of pristine graphene sheet under uniaxial tension along armchair and zigzag directions at different temperatures (300~900 K).

Our MD simulation results demonstrated that both S-W defects and temperature could significantly deteriorate the fracture strength of graphene. Figure 2 showed the fracture strength of graphene with S-W defects at different temperatures (300 K ~ 900 K). Under zigzag loading, the average strength loss caused by S-W_1 and S-W_2 was 16.26% and 41.30%, respectively. Under armchair loading, the average loss of facture strength by S-W_2 defect was about 15.75%. For S-W_1, however, fracture strength increased when temperature was above 600 K (C point in Figure 2(a)). This was attributed to the healing of S-W_1 defect with increasing temperature. As shown in Figure 2(b), at 600 K, the S-W_1 defect was stable. At 700 K, however, the S-W_1 defect was healed by 90° rotation of C-C bond. As mentioned above, mechanical strain could lower the healing energy barrier E_{eb}^{-}. Therefore, according to the kinetic rate of the healing of S-W defects (ν),

$$\nu = af_0 \exp^{-E_{eb}^{-}/kT} \quad (1)$$

Where f_0 is attempt frequency (about 10^{13}/s); k is the Boltzmann's constant and a is the lattice spacing $a = \sqrt{3}r_0$, where $r_0 = 1.42$ Å is the C-C bond length. From Eq. 1, the healing of S-W_1 defect became easier with increase of mechanical strain and temperature, consistent with the MD simulation.

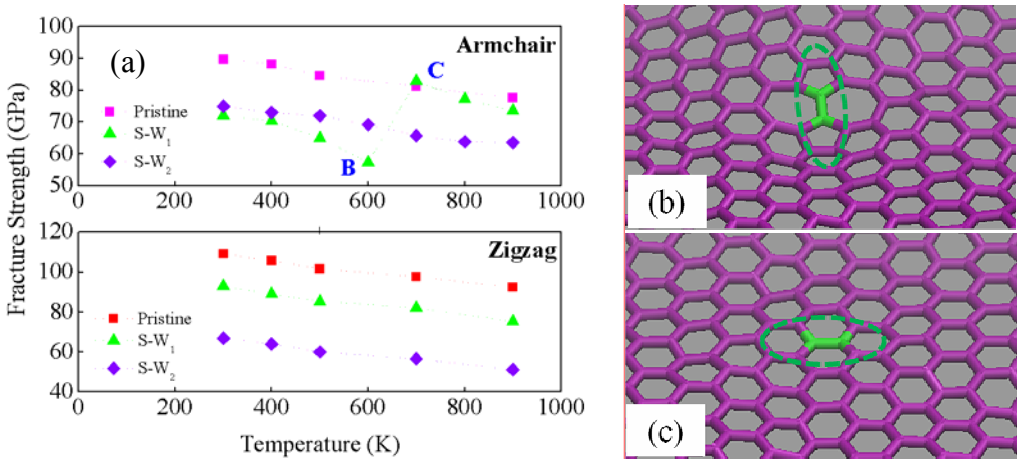

Figure 2. (a) Fracture strength of pristine, S-W_1 and S-W_2 defected graphene versus temperature under armchair and zigzag loading conditions. (b-c) Configuration change in the pre-existing S-W_1

defect from point B (b) (at 600 K) to point C (c) (at 700 K) highlighted in (a).

3.2 Effect of Vacancy Defect on Fracture Strength

In the temperature range of 300~900 K, the fracture strength of graphene sheet with vacancy was evaluated under tension along the armchair direction. The simulation model with 1, 2, and 3 vacancies is shown in Figure 3(a). Figure 3(b) showed the fracture strength σ_f for the graphene sheets with different vacancy number at temperatures 300 K, 500 K, and 900 K. It can be seen that fracture strength decreases with increasing temperature as well as the number of vacancy. For the sheet with 3 vacancies, the fracture strength loss was 37.3%, 40.2% and 42.4%, corresponding to 300, 500 and 900 K, respectively. Therefore, atomic scale defect such as vacancy does play a critical role in dictating the mechanical performance of graphene.

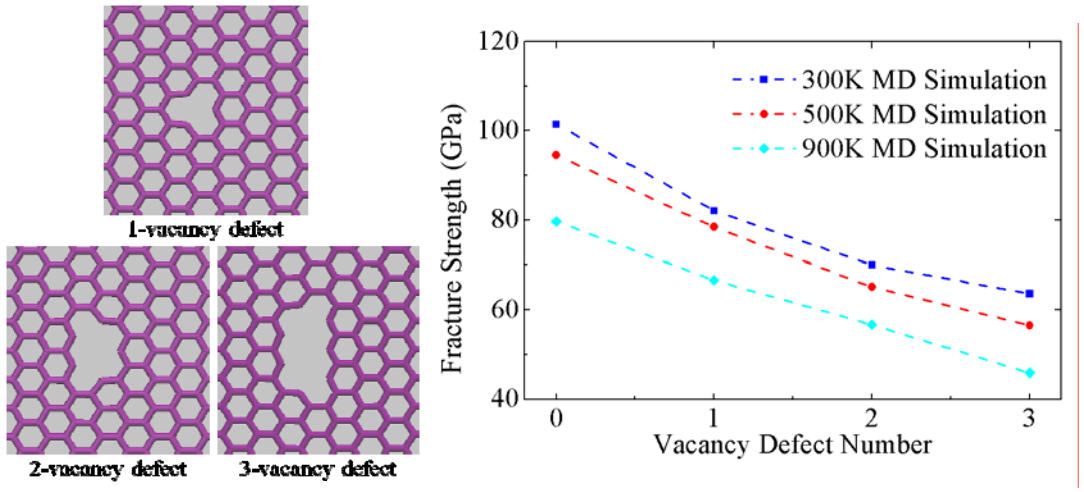

(a) **(b)**

Figure 3. (a) Three types of vacancy defect. (b) Fracture strength of defective graphene sheet versus the number of vacancy defect.

3.3 Interfacial Behaviour of Graphene-PE Nanocomposites

To study the interfacial behavior of graphene-PE nanocomposites, MD simulation of pull-out test was carried out by pulling out the graphene nanofiller from PE matrix. In particular, interfacial shear force (ISF) can govern the effectiveness of load transfer during pull-out process. On the basis of the expressions $f_{ISF} = -\partial E_{\text{int}} / \partial X$, f_{ISF} can be calculated in terms of the given E_{int}-X curve. As shown in Figure 4(a), f_{ISF}-X curve can also be divided into three stages. It can be found that the Stage I and Stage III had approximately the same range of X_I=X_{III}=1.0 nm, which was close to the cut-off distance of vdW interaction. At Stage I, the magnitude of f_{ISF} rose quickly in all cases. The increase of f_{ISF} can be attributed to the newly formed surface of graphene (outside part). Then, f_{ISF} went through a long and approximate platform at Stage II. This was because that the length of the effective newly formed surface kept at 1 nm from the pull-out end, thus leading to constant f_{ISF}. Finally, it decreased to the value similar to that at first beginning until complete pull-out. At all three stages, the values of f_{ISF} varied periodically with the variation of X, largely due to the inhomogeneous distribution of PE structures in the interfacial area. The effect of structural defect on f_{ISF} was considered as well. However, the effect of structural defects on f_{ISF} is unobvious, which might be beneficial for application of graphene-polymer nanocomposites. Then, pull-out stress could be calculated in the expression as σ_p=f_{ISF}/A_{eff}, where A_{eff} is the effective cross section of graphene sheet, A_{eff}=Wt with W=50 Å the width of graphene sheet and t=3.44 Å the sheet thickness.

According to Figure 4, the maximum pull-out stress $\sigma_p^{\max}$ in both cases was about 0.87 GPa, much lower than fracture strength of pure graphene and defective graphene, namely $\sigma_p^{\max} / \sigma_f = 1$. Therefore, in the pratical applications of graphene-polymer nanocomposites, graphene nanofiller could be full utilized even with structural defects on its surface. However, increasing the utilization of fracture strength of graphene deserves further investigation in future.

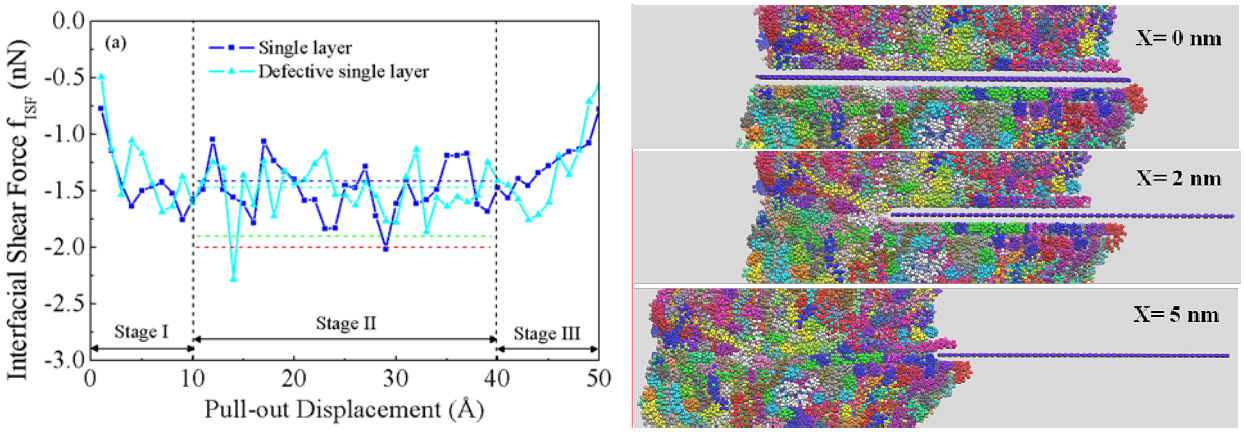

(a) (b)

Figure 4. (a) Interfacial shear force f_{ISF} versus pull-out displacement X in Case 1 (pure graphene sheet) and Case 2 (defective graphene sheet). (b) Snap shots of graphene pull-out from PE matrix in Case 1.

4. Conclusions

Deformation and failure of graphene sheet and graphene-polymer interface was investigated using MD simulations. Calculation results showed that the fracture strength of graphene is dependent on both structural defects and temperature. Structural defects in graphene (e.g. Stone-Wales defect and multi-vacancy defect) can remarkably damage the fracture strength of graphene. As for the interfacial behaviour of graphene-polymer nanocomposites, it was shown that the value of ISF vary at each end of the graphene nanofiller within the range of 1 nm, while keep approximately constant (ISF) and zero (ISS) at middle stage. Particularly, ISF is independent of the pre-existing vacancy defect in graphene. Furthermore, graphene nanofiller could be full utilized even with structural defects owing to much lower pull-out stress. The study of the mechanical performance of defective graphene and graphene-polymer interface sheds light on the better understanding of design and application of graphene-polymer nanocomposites.

References

[1] K. S. Novoselov, A. K. Geim, S. V. Morozov, D. Jiang, Y. Zhang, S. V. Dubonos, I. V. Grigorieva and A. A. Firsov, Electric field effect in atomically thin carbon films. Science, 306 (2004) 666.

[2] Y. Zhang, Y.-W. Tan, H. L. Stormer and P. Kim, Experimental observation of the quantum Hall effect and Berry's phase in graphene. Nature (London), 438 (2005) 201.

[3] C. Lee, X. Wei, J. W. Kysar and J. Hone, Measurement of the elastic properties and intrinsic strength of monolayer graphene. Science, 321 (2008) 385.

[4] A. A. Balandin, S. Ghosh, W. Bao, I. Calizo, D. Teweldebrhan, F. Miao and C. N. Lau, Superior Thermal Conductivity of Single-Layer Graphene. Nano Lett, 8 (2008) 902.

[5] S. Stankovich, D. A. Dikin, G. H. B. Dommett, K. M. Kohlhaas, E. J. Zimney, E. A. Stach, R. D.

Piner, S. T. Nguyen and R. S. Ruoff, Graphene-based composite materials. Nature, 442 (2006) 282.
[6] RamanathanT, A. A. Abdala, StankovichS, D. A. Dikin, M. Herrera Alonso, R. D. Piner, D. H. Adamson, H. C. Schniepp, ChenX, R. S. Ruoff, S. T. Nguyen, I. A. Aksay, R. K. Prud'Homme and L. C. Brinson, Functionalized graphene sheets for polymer nanocomposites. Nat Nanotechnol, 3 (2008) 327.
[7] M. A. Rafiee, J. Rafiee, Z. Z. Yu and N. Koratkar, Buckling resistant graphene nanocomposites. Appl Phys Lett, 95 (2009) 223103.
[8] M. A. Rafiee, J. Rafiee, Z. Wang, H. Song, Z.-Z. Yu and N. Koratkar, Enhanced mechanical properties of nanocomposites at low graphene content. ACS Nano, 3 (2009) 3884.
[9] X. Zhao, Q. Zhang, D. Chen and P. Lu, Enhanced Mechanical Properties of Graphene-Based Poly(vinyl alcohol) Composites. Macromolecules, 43 (2010) 2357.
[10] M. A. Rafiee, J. Rafiee, I. Srivastava, Z. Wang, H. H. Song, Z. Z. Yu and N. Koratkar, Fracture and Fatigue in Graphene Nanocomposites. Small, 6 (2010) 179.
[11] M. A. Rafiee, W. Lu, A. V. Thomas, A. Zandiatashbar, J. Rafiee, J. M. Tour and N. A. Koratkar, Graphene nanoribbon composites. ACS Nano, 4 (2010) 7415.
[12] I. Srivastava, R. J. Mehta, Z.-Z. Yu, L. Schadler and N. Koratkar, Raman study of interfacial load transfer in graphene nanocomposites. Appl Phys Lett, 98 (2011) 063102.
[13] P. R. Somani, S. P. Somani and M. Umeno, Planer nano-graphenes from camphor by CVD. Chem Phys Lett, 430 (2006) 56.
[14] A. A. Green and M. C. Hersam, Solution phase production of graphene with controlled thickness via density differentiation. Nano Lett, 9 (2009) 4031.
[15] V. Singh, D. Joung, L. Zhai, S. Das, S. I. Khondaker and S. Seal, Graphene based materials: Past, present and future. Prog Mater Sci, 56 (2011) 1178.
[16] F. OuYang, B. Huang, Z. Li, J. Xiao, H. Wang and H. Xu, Chemical functionalization of graphene nanoribbons by carboxyl groups on Stone-Wales defects. J Phys Chem C, 112 (2008) 12003.
[17] D. W. Boukhvalov and M. I. Katsnelson, Chemical functionalization of graphene. J Phys-Condens Mat, 21 (2009) 344205.
[18] M. Wu, X. Wu, Y. Gao and X. C. Zeng, Materials design of half-metallic graphene and graphene nanoribbons. Appl Phys Lett, 94 (2009) 223111.
[19] A. J. Stone and D. J. Wales, Theoretical-studies of icosahedral C60 and some related species. Chem Phys Lett, 128 (1986) 501.
[20] N. Gorjizadeh, A. A. Farajian and Y. Kawazoe, The effects of defects on the conductance of graphene nanoribbons. Nanotechnology, 20 (2009) 015201.
[21] Q. X. Pei, Y. W. Zhang and V. B. Shenoy, Mechanical properties of methyl functionalized graphene: a molecular dynamics study. Nanotechnology, 21 (2010) 115709.
[22] Q. X. Pei, Y. W. Zhang and V. B. Shenoy, A molecular dynamics study of the mechanical properties of hydrogen functionalized graphene. Carbon, 48 (2010) 898.
[23] Y. Li, Y. Liu, X. Peng, C. Yan, S. Liu and N. Hu, Pull-out simulations on interfacial properties of carbon nanotube-reinforced polymer nanocomposites. Comp Mater Sci, 50 (2011) 1854.
[24] G. Yamamoto, S. Liu, N. Hu, T. Hashida, Y. Liu, C. Yan, Y. Li, H. Cui, H. Ning and L. Wu, Prediction of pull-out force of multi-walled carbon nanotube (MWCNT) in sword-in-sheath mode. Comp Mater Sci, 60 (2012) 7.

[25] Alamusi, N. Hu, B. Jia, M. Arai, C. Yan, J. Li, Y. Liu, S. Atobe and H. Fukunaga, Prediction of thermal expansion properties of carbon nanotubes using molecular dynamics simulations. Comp Mater Sci, 54 (2012) 249.
[26] M. C. Wang, C. Yan, L. Ma, N. Hu and M. W. Chen, Effect of defects on fracture strength of graphene sheets. Comp Mater Sci, 54 (2012) 236.
[27] M. C. Wang, C. Yan, L. Ma and N. Hu, Molecular dynamics investigation on edge stress and shape transition in graphene nanoribbons. Comp Mater Sci, 68 (2013) 138.
[28] H. Zhao, K. Min and N. R. Aluru, Size and Chirality Dependent Elastic Properties of Graphene Nanoribbons under Uniaxial Tension. Nano Lett, 9 (2009) 3012.
[29] W. G. Hoover, Canonical dynamics: Equilibrium phase-space distributions. Phys Rev A, 31 (1985) 1695.
[30] S. Nosé, A unified formulation of the constant temperature molecular dynamics methods. J Chem Phys, 81 (1984) 511.
[31] S. J. Stuart, A. B. Tutein and J. A. Harrison, A reactive potential for hydrocarbons with intermolecular interactions. J Chem Phys, 112 (2000) 6472.
[32] S. Plimpton, Fast parallel algorithms for short-range molecular dynamics. J Comput Phys, 117 (1995) 1.
[33] H. Sun, Ab initio characterizations of molecular structures, conformation energies, and hydrogen-bonding properties for polyurethane hard segments. Macromolecules, 26 (1993) 5924.
[34] H. Sun, S. J. Mumby, J. R. Maple and A. T. Hagler, An ab Initio CFF93 All-Atom Force Field for Polycarbonates. J Am Chem Soc, 116 (1994) 2978.
[35] I. Yarovsky and E. Evans, Computer simulation of structure and properties of crosslinked polymers: application to epoxy resins. Polymer, 43 (2002) 963.
[36] T. C. Clancy and T. S. Gates, Modeling of interfacial modification effects on thermal conductivity of carbon nanotube composites. Polymer, 47 (2006) 5990.
[37] M. Naito, K. Nobusawa, H. Onouchi, M. Nakamura, K.-i. Yasui, A. Ikeda and M. Fujiki, Stiffness- and Conformation-Dependent Polymer Wrapping onto Single-Walled Carbon Nanotubes. J Am Chem Soc, 130 (2008) 16697.
[38] J. Lee, V. Varshney, J. S. Brown, A. K. Roy and B. L. Farmer, Single mode phonon scattering at carbon nanotube-graphene junction in pillared graphene structure. Appl Phys Lett, 100 (2012) 183111.
[39] L. Hu, T. Desai and P. Keblinski, Determination of interfacial thermal resistance at the nanoscale. Phys Rev B, 83 (2011) 195423.
[40] S. Yang, S. Yu, W. Kyoung, D.-S. Han and M. Cho, Multiscale modeling of size-dependent elastic properties of carbon nanotube/polymer nanocomposites with interfacial imperfections. Polymer, 53 (2012) 623.
[41] E. Zaminpayma and K. Mirabbaszadeh, Interaction between single-walled carbon nanotubes and polymers: A molecular dynamics simulation study with reactive force field. Comp Mater Sci, 58 (2012) 7.